

Alma Mater Studiorum Università di Bologna
Archivio istituzionale della ricerca

How to transform a fixed stroke alternating syringe ventricle into an adjustable elastance ventricle

This is the final peer-reviewed author's accepted manuscript (postprint) of the following publication:

Published Version:

Corazza, I., Casadei, L., Bonafè, E., Cercenelli, L., Marcelli, E., Zannoli, R. (2018). How to transform a fixed stroke alternating syringe ventricle into an adjustable elastance ventricle. *REVIEW OF SCIENTIFIC INSTRUMENTS*, 89(7), 074301-1-074301-8 [10.1063/1.5030100].

Availability:

This version is available at: <https://hdl.handle.net/11585/638560> since: 2018-07-24

Published:

DOI: <http://doi.org/10.1063/1.5030100>

Terms of use:

Some rights reserved. The terms and conditions for the reuse of this version of the manuscript are specified in the publishing policy. For all terms of use and more information see the publisher's website.

This item was downloaded from IRIS Università di Bologna (<https://cris.unibo.it/>).
When citing, please refer to the published version.

(Article begins on next page)

How to transform a fixed stroke alternating syringe ventricle into an adjustable elastance ventricle

Ivan Corazza, Lorenzo Casadei, Elisa Bonafè, Laura Cercenelli, Emanuela Marcelli, Romano Zannoli

Experimental, Diagnostic and Specialty Medicine Department, University of Bologna, Bologna Italy

Corresponding author:

Ivan Corazza

DIMES, University of Bologna

Via Massarenti, 9

40138 Bologna

Italy

Phone: +39 051 2143588

Mail: ivan.corazza@unibo.it

Keywords

End-systolic pressure-volume relationship, cardiovascular mock, variable elastance, P-V loops

Short title: From a fixed stroke to a adjustable elastance ventricle simulator

Abstract

Most devices used for bench simulation of the cardiovascular system are based either on a syringe-like alternating pump or an elastic chamber inside a fluid-filled rigid box. In these devices it is very difficult to control the ventricular elastance and simulate pathologies related to the mechanical mismatch between ventricle and arterial load (i.e. heart failure). This work presents a possible solution to transforming a syringe-like pump with a fixed ventricle into a ventricle with variable elastance.

Our proposal was tested in two steps: (1) fixing the ventricle and the aorta and changing the peripheral resistance (PHR); (2) fixing the aorta and changing the ventricular elastance and the PHR. The signals of interest were acquired to build the ventricular pressure-volume (P-V) loops describing the different physiological conditions and the end-systolic pressure-volume relationships (ESPVR) were calculated with linear interpolation.

The results obtained show a good physiological behavior of our mock for both steps. (1) Since the ventricle is the same, the systolic pressures increase and stroke volumes decrease with the PHR: the ESPVR, obtained by interpolating the pressure and volume values at end-systolic phases, is linear. (2) Each ventricle presents ESPVR with different slopes depending on the ventricle elastance with a very good linear behavior.

In conclusion, this paper demonstrates that a fixed stroke alternating syringe ventricle can be transformed into an adjustable elastance ventricle.

Keywords

End-systolic pressure-volume relationship, cardiovascular mock, variable elastance, P-V loops

Introduction

Recent years have seen an ongoing interest in biomechanical interventions designed to improve or recover cardiovascular function, and many new implantable devices have been developed, evaluated and introduced into clinical practice. Innovative cardiac valves (transcatheter aortic valve implantation, TAVI), left ventricular assist devices (LVAD), ventricular and vascular biomechanical interventions (endovascular aortic repair, EVAR) increasingly represent an elective solution for many different cardiovascular pathologies ¹⁻⁸.

Research and innovation, starting from an idea and ending with implantation of the device, is a long and expensive process comprising an in-depth analysis of biocompatible materials, prototype realization, numerical simulation, in-vitro testing and then animal and human experimentation. In this difficult but necessary course of research, in-vitro testing represents an increasingly important step. Good mechanical testing can help the numerical simulation and yield important suggestions for prototype optimization and in-vivo experimentation. Accurate functional and mechanical computer simulation of a device's behavior in different operative conditions is essential to guide the research process in the right direction ^{9,10}, but optical observation and direct measurement on a mechanical prototype is more convincing. For this reason, many mechanical simulators of the cardiovascular system varying in complexity and approach (syringe-like, elastic chamber inside a fluid-filled rigid box, etc.) have been developed and are currently used both for teaching and research ¹¹⁻²². Nevertheless, the paucity and cost of standardized cardiovascular commercial mocks (e.g., VivitroSuperPump, ViVitro Labs, Victoria, BC, Canada) have stimulated a continuous process of innovation and proposals aimed at overcoming the functional limitations of existing solutions.

The mechanical behavior of a ventricle and its coupling with its atrial preload and arterial load was first described by the time-varying elastance theory ²³⁻²⁶. In recent years, the model has been clinically validated in different cardiological and cardiovascular diseases ^{27,27-36} and now constitutes the theoretical background necessary to build a reliable mechanical simulator of the cardiovascular system.

The easiest way to build a mechanical ventricle is to use an alternating syringe with two unidirectional valves. When the stroke volume (SV) of this pump is transferred into an elastic wall chamber connected to a hydraulic resistance pipeline, a physiologically shaped

arterial pressure pulse can be obtained, which changes by adjusting the syringe stroke, the volume and elasticity of the chamber and the hydraulic resistance of the line.

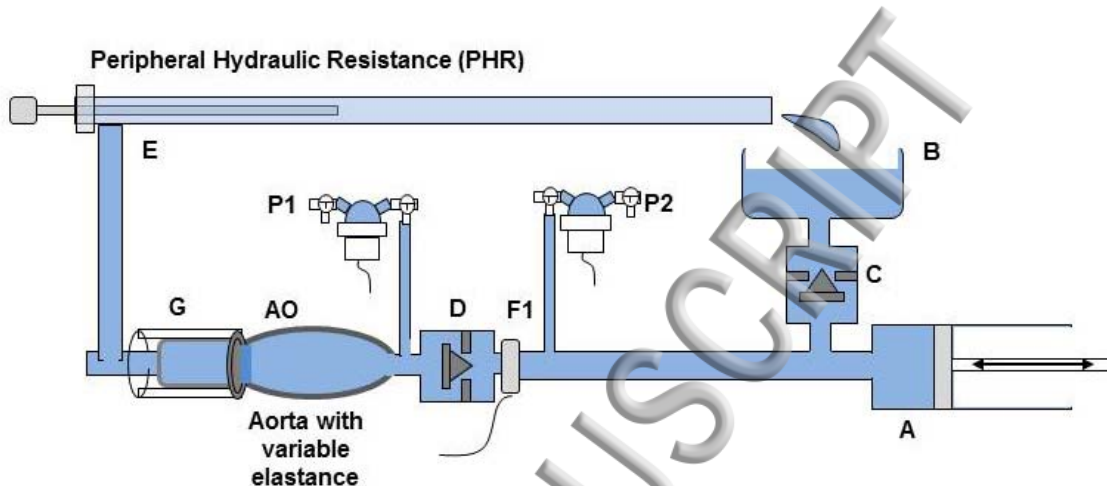


Fig. 1. Simple mechanical mock of the cardiovascular system with fixed stroke volume. (A) Syringe connected to an alternating pump to simulate the left ventricle; (B) Left atrium; (C) Mitral valve; (D) Aortic valve; (AO) Aorta; (E) Rubber tube with an internal movable catheter to simulate the hydraulic peripheral resistance; (F1) Electromagnetic flowmeter to measure the aortic flow (AF); (P1) Pressure transducer to measure the aortic pressure (AP); (P2) Pressure transducer to measure the ventricular pressure (VP). The aortic elastance can be modified through a rigid plastic tube (G) which can be progressively placed around the aortic rubber tube (AO).

This system is used for many vascular simulations (i.e. studies on the mechanical behavior of cardiac valves) but it does not accurately reproduce the different matching conditions between a physiologic ventricle and an arterial system, with consequent energy management. In fact, the time variable ventricular elastance theory connects the energy transfer from the ventricle to the artery to the instantaneous ventricular and arterial elastances^{25,26,33,37}. The instantaneous ventricular elastance changes over time and in a normal heart provides the best matching conditions in terms of energy transfer. Since the arterial elastance is passive and depends on the elastic properties of the walls, the best matching condition can be physiologically reached only by changes in ventricular behavior. For example, if the aorta stiffens (with hypertension), the left ventricle increases its elastance becoming hypertrophic^{27,28,32,34,35}. If the changes in arterial elastance are

pathologic and, for example, elastance suddenly increases, the ventricle will not be able to follow the changes and a mismatch condition is reached (i.e. aortic dissection)^{31,34,36,38}.

In addition, a pathological change in ventricular contractile function (i.e. heart failure, cardiac dilatation, etc.) may generate a mismatch between the pump and a normal arterial load. In this case, the ventricle tries to adapt its contractile behaviour to the normal aorta but the only outcome is progression of the mismatch and a worse prognosis^{29,30}.

Inotropic drugs are commonly used in clinical practice to modify ventricular contractility. If the effect is positive, the ventricular ESPVR changes, ventricular elastance increases and aorto-ventricular matching improves. If the effect is negative, the ESPVR slope decreases and aorto-ventricular matching tends to worsen³⁹. All this clinical evidence demonstrates that ventricular elastance changes in relation to specific drugs, ventricular pathology and shifts in arterial elastance.

For these reasons, the simple setup described in Fig. 1 cannot adequately mimic all these aspects in many important physiological conditions (i.e. arterial dissection, arterial hypertension, heart failure (HF), cardiogenic shock, positive or negative inotropic drug therapy, etc.) since the ventricular elastance is not adjustable. To approximate real situations, we can use tubes of different shapes, size and elasticity to improve the reproduce the elastance of an arterial system, but it is very difficult to build pumping systems with ventricular-like instantaneous elastances.

In some cases, the ventricle is made of a chamber filled with liquid surrounded by air: the ventricular elastance can be adjusted by controlling the external air pressure and volume separately from the pumping function. To do this, motors and valves and an external electronic device must be added to the mock pumps to properly control these additional parts^{16-19,21,22,40,41}. Moreover, the elastance may also be changed according to physiological values previously acquired from patients, and the Frank Starling mechanism simulated.

These solutions need programmable modules (i.e. microprocessors, computers, etc.) to drive the pump on the basis of previously established (theoretically or clinically) elastance curves. This approach gives good results in terms of the correspondence between the set and experimental variable elastances, but needs an active computer-based control system that can be expensive and difficult to program.

A previous paper of ours⁴² described a simple system where an external chamber applied to the alternating syringe core permitted a sort of mechanical feedback to change the SV

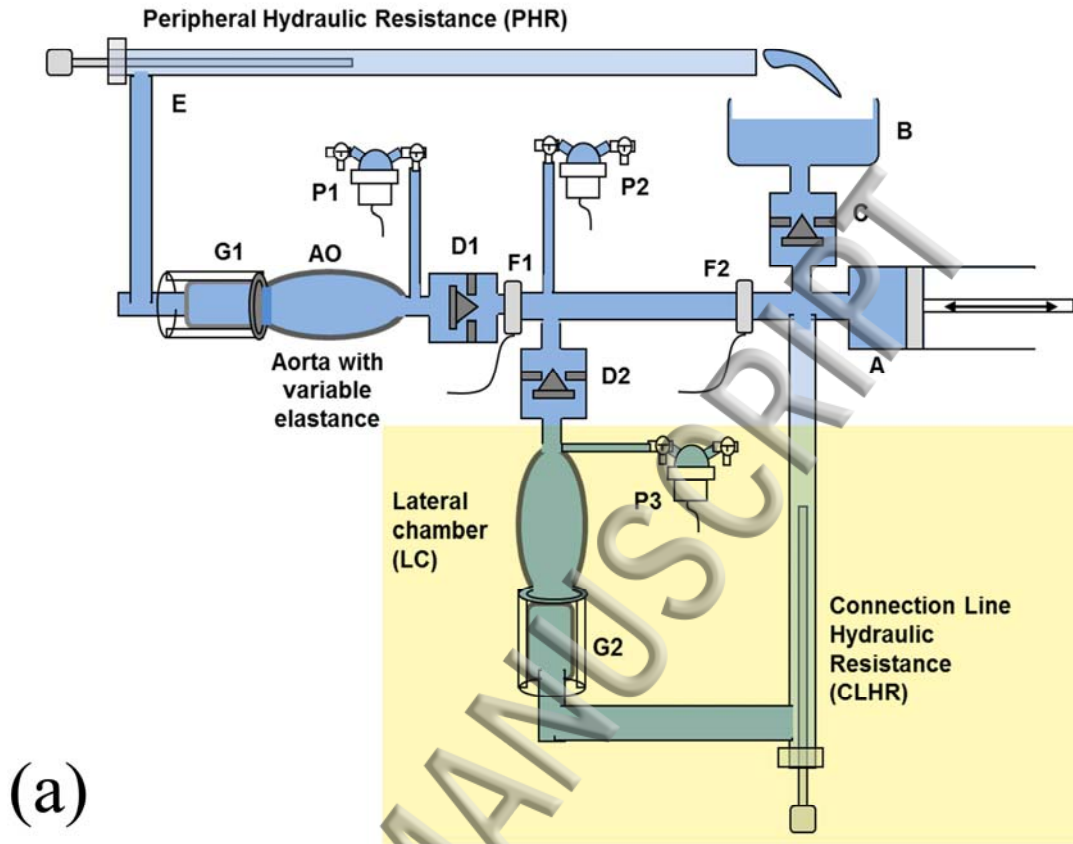
and regulate the matching between the pump and the elastic load. The limit of this solution was the impossibility to change the mechanical behavior (the elastance) of the ventricle in a continuous way. By changing preload or afterload, the PV loops obtained differed but the ESPVR was the same in all the simulated conditions.

From that first prototype we moved to a new solution described in this paper which permits a more flexible operation with continuous regulation. This setup allows the ventricular elastance to be adjusted continuously from the condition of a fixed stroke syringe (infinite elastance) to very low elastance values simulating ventricular HF, cardiac rupture or massive infarct (very low elastance) and also to simulate and analyze the mechanical matching or mismatching between ventricle and artery. This is not the final solution: additional technical interventions have to be introduced to obtain a ventricular mock adequately simulating a physiological system.

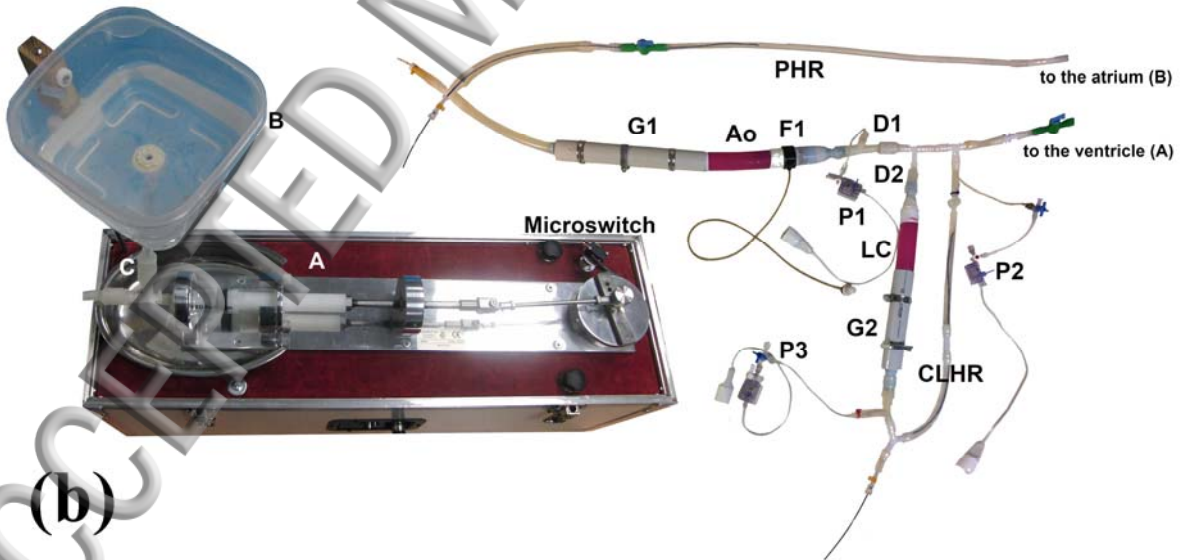
Material and methods

The proposal is based on two solutions: 1) how to change a fixed stroke pumping syringe system into a variable stroke one; 2) how to obtain adjustable elastance conditions of the pump and, consequently, load matching-related variable strokes.

The solution concept is similar to that tested in previous papers⁴²⁻⁴⁴: an elastic chamber of selected elasticity (volume, material and wall thickness) is connected to the syringe output in parallel with the arterial line. To avoid continuous back flow exchange between the chamber and the syringe during diastole, a unidirectional valve was put on the lateral chamber entrance and a variable resistance line was back connected to the syringe output (Fig. 2).



(a)



(b)

Fig. 2. (a) Mechanical mock of the cardiovascular system with variable ventricular elastance and stroke volume and (b) picture of the system in use. (A) Syringe; (LC) Lateral ventricular chamber; (B) Left atrium; (C) Mitral valve; (D1) Aortic valve; (E) Hydraulic peripheral resistance; (F1) Electromagnetic flowmeter to measure AF; (P1) Pressure transducer to measure AP; (P2) Pressure transducer to measure VP; (D2) Valve to prevent back flow during diastole; (P3) Pressure transducer to measure the pressure of the lateral

chamber (LC). Both the aortic and ventricular elastances can be modified through rigid plastic cylinders (G1, G2), which can be progressively placed around the aortic rubber tube and the lateral ventricular chamber. The connection line hydraulic resistance (CLHR) allows the pressures in the aorta and lateral chamber to be balanced.

The CLHR line is necessary for the lateral chamber to empty during diastole. With this apparently complex setup the aortic valve closes at the end of syringe ejection, and the time constant of the arterial pressure decay depends only on the arterial elastance and PHR. During the filling phase, the syringe receives flow from the reservoir simulating the atrium and from the lateral chamber line, depending on the lateral chamber pressure (LCP) and connection line hydraulic resistance (CLHR). The CLHR should be adjusted to have the same pressure in the artery as the lateral chamber, at the start of ejection. That means having the same time constant of the artery and the lateral chamber, but with different compliances. This is obtained by regulating the CLHR. For a continuous and accurate regulation of the hydraulic resistance of the connection line we used the solution shown in Fig. 2.

With the described setup we obtained a ventricle with an adjustable elastance and an arterial load with specific elastance and PHR. We can easily measure the physical work transferred (W_t) to the artery by the arterial pressure (AP) and flow (AF) product integral (eq 1) and the work produced by the syringe (W_p) and the pressure-flow (SP, SF) product at the syringe output (eq 2). A transducer measures the pressure while an electromagnetic transducer placed after the syringe acquires the flow. The transferred and produced work comparison shows how the efficiency (ϵ) of energy production and transfer changes by adjusting the lateral chamber elastance (ventricle), arterial elastance and the PHR (eq 3).

$$(eq\ 1)\ W_t = \int AP(t) \cdot AF(t) \cdot dt$$

$$(eq\ 2)\ W_p = \int SP(t) \cdot SF(t) \cdot dt$$

$$(eq\ 3)\ \epsilon = \frac{W_t}{W_p}$$

Considering the syringe and the lateral chamber as basic components of the mechanical ventricle, the instantaneous ventricular volume is the sum of the instantaneous lateral chamber volume (LCVol) plus the syringe volume (SVol), paying attention to operate in a limited pressure range, where the arterial elastance and the elastance of the lateral chamber can be assumed to be constant. We can obtain the P-V loop by starting from the

ejection starting point and measuring the corresponding pressure, SVol and LCVol. The subsequent pressure and volume points of the P-V loop can be obtained by directly measuring the ventricular pressure (VP) and calculating the ventricular volume (VVol) as the sum of the instantaneous measurement of the LCVol and SVol.

This setup can verify if the mock accomplishes the Suga–Sagawa linear ESPVR ^{23,25,37}. For this it should be sufficient to operate the system, adjust the peripheral arterial resistance and see if the left upper corners of the P-V curves obtained stay on a straight line. If they do, the mock can be claimed to simulate the physiological behavior of a ventricle. But the most important innovation of the proposal is the possibility to simulate different ventricular elastances, and the linear ESPVR test must be repeated by changing the ventricular elastance from a condition of ventricular fixed stroke (infinite elastance) to a condition of arterial pressure and flow reduction due to impaired ventricular elastance, described by the change in the ESPVR slope.

An alternating 50 mL syringe system with fixed 22 mL normal saline SV was used. Three different pressure sensors (Baxter, Edwards, TrueWave) were used to measure the aortic pressure (AP), VP and LCP. The syringe fixed flow (SFF) was measured with a standard electromagnetic flowmeter (BL610 flowmeter 8mm, Biotronex Lab, Chester, MD, USA). All these analog signals were then conditioned, sampled at 1KHz with a resolution of 12bit, stored and analyzed with a commercial device (Anscovary System, Sparkbio Srl, Bologna, Italy) ⁴⁵.

The LCVol was measured in real time with a modified Simpson method applied to a video acquisition made with a digital camera (EX-SH20, Casio Computers Co., Tokyo, Japan) ⁴⁶. Since the camera works at 30fps, the LCVol was sampled at that rate, the ventricular pressure signals acquired with the Anscovary System were down-sampled at 30Hz with a cubic spline interpolation before building the P-V loops.

The experimental protocol was divided into two main steps. The first was to verify the existence of a linear ESPVR by changing the PHR and maintaining the same ventricle and aorta. Six different conditions were set by changing the position of the cursor PHR with a fixed heart rate (HR) of 60 bpm. The second step was to simulate three different conditions of ventricular elastance by acting on the G2 rigid tube (Fig. 3a) and setting three PHR values for each condition (Fig. 3b) calculating three ventricular elastance-related P-V loops. HR was fixed at 60bpm.

For each simulated condition, the resistance of the hydraulic connection of CLHR was also set to obtain the same pressure values for AP and LCP at the start of ejection.

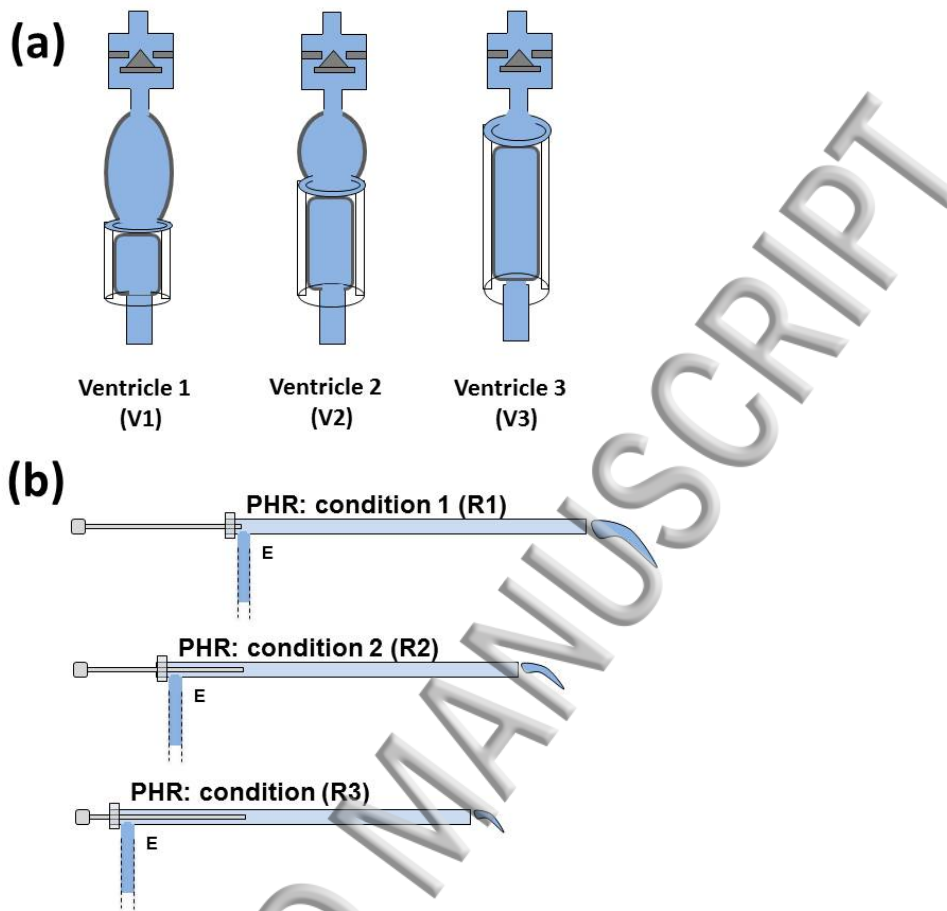


Fig. 3. (a) Different conditions of ventricular elastance, ranging from V1 (lowest elastance) to V3 (completely stiff rigid tube) obtained by changing the position of the rigid plastic tube around the lateral chamber. (b) Three peripheral resistances (R1, R2, R3) obtained by changing the insertion length of the catheter inside the peripheral vessel.

For each condition of both steps, the following parameters were calculated:

1) *Ventricular volume (VVol)*: t was evaluated by summing the instantaneous values of LCVol and SVol (obtained by integrating the syringe flow curves). The volume of the water inside the rigid tubes, stopcocks and connections inside the ventricle is constant and was neglected.

2) *Systolic, diastolic and mean aortic pressure (SAP, DAP, MAP)*: for each condition, ten cardiac cycles were considered and the signals of interest (AP and VP and SFF) mediated

to obtain a more representative wave. Then SAP, DAP and MAP were measured together with their statistical errors (standard deviations).

3) SV was calculated as the difference between the end-systolic and end-diastolic volumes.

4) PHR was calculated as the ratio between the mean aortic pressure less the atrial one and mean aortic flow. Since the difference in height (h) between the atrium (Figs. 2a-B, 2b-B) and the aorta (figs 2a-AO, 2b-AO) is fixed at 20cm, the atrial pressure (ρgh , where ρ =density of water and g = gravity acceleration) results 15mmHg.

5) ESPVR was calculated as the best line interpolating all end-systolic points on the P-V loops. A squared Pearson's coefficient (R^2) higher than 0.8 was considered significant to demonstrate a good linear trend of the ESPVR and a consequent positive outcome for our model.

Results

An example of the analog signals obtained by the mock is shown in Fig. 4. The shapes of the waves are physiological, but since the pressure transducers are next to the aortic valve the pressure signals present some noise coinciding with the valve movements. This high-frequency noise does not affect the measurements of interest.

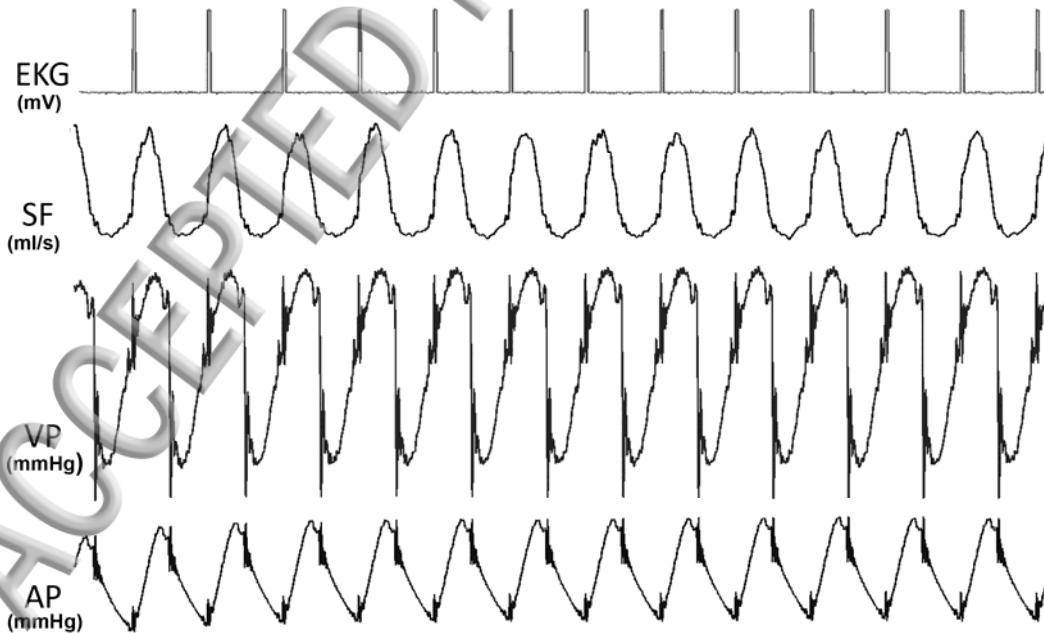


Fig. 4. Example of signals (EKG, syringe flow, ventricular and aortic pressure) acquired with the Ansccovery System (SparkBio Srl). EKG was generated through a microswitch connected to the syringe. Since the

system comprises valves, transducers, tubes of different diameter and bifurcation, the acquired signals present some noise and irregular shapes due to local vortex and reflections. Since these artifacts are random, they disappear after the mediation of ten cardiac cycles.

AP, SV and vascular resistances for the six conditions of step 1 are shown in Table 1.

Case	PHR (mmHg s /ml)	Systolic Pressure (mmHg)	Diastolic Pressure (mmHg)	Mean Pressure (mmHg)	SV (ml)
1	4.73	112±1	76±1	87±4	15.4±0.2
2	5.07	119±2	77±2	91±3	15.0±0.2
3	5.28	125±2	78±1	93±4	14.8±0.1
4	7.05	150±3	102±3	118±5	14.5±0.2
5	9.34	177±4	130±4	145±5	13.9±0.2
6	10.71	189±3	147±3	161±4	13.6±0.1

Table 1 Systolic, diastolic and mean pressures, stroke volumes and peripheral resistances for the six different simulated conditions.

The six ventricular pressure curves measured and used for P-V loop construction of step 1 are shown in Fig. 5a. The six ventricular “volumes” calculated for the six conditions of step 1 are shown in Fig. 5b.

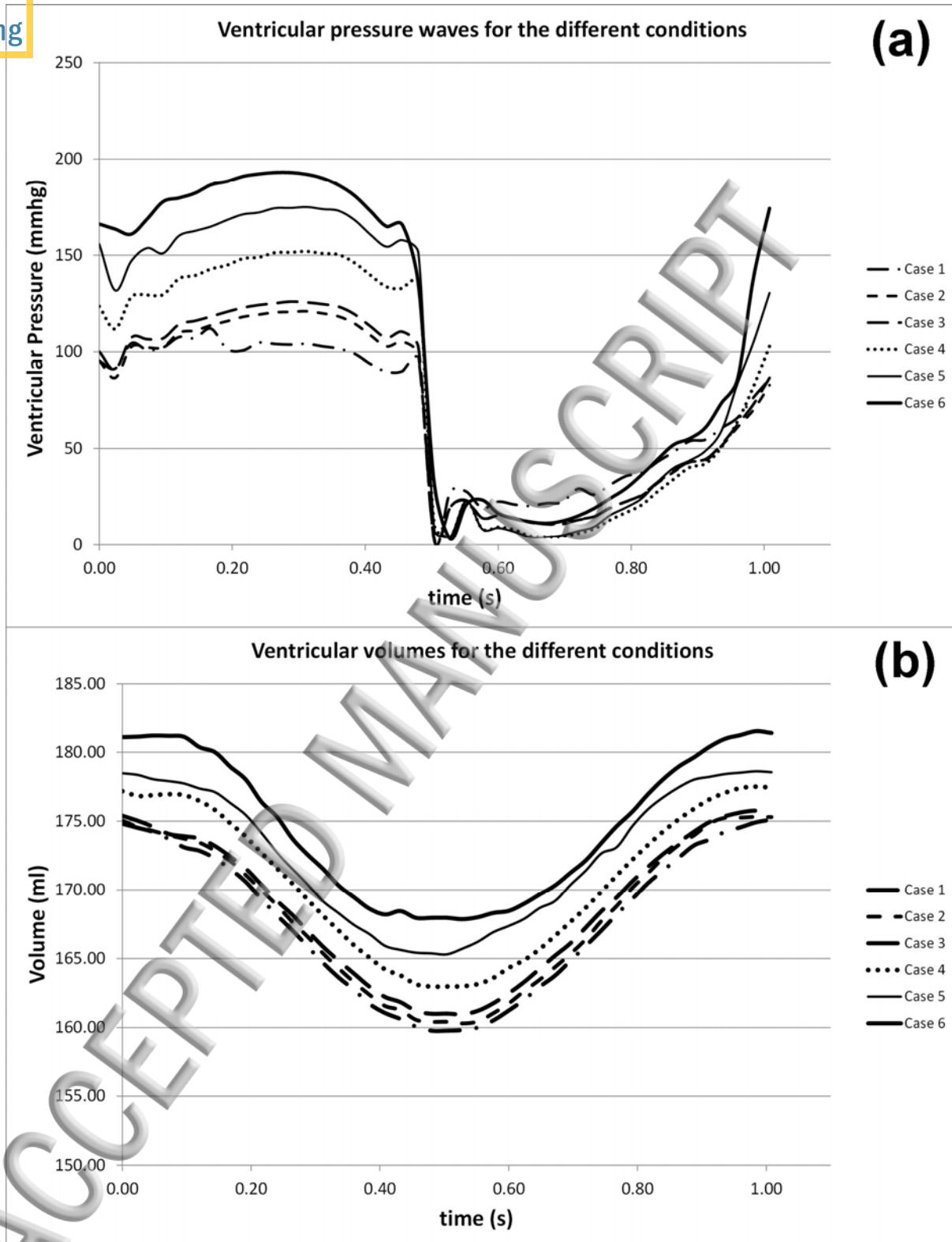


Fig. 5. (a) Ventricular pressure waves corresponding to the different conditions of PHR. The systolic pressure increases with increasing PHR. The minimal ventricular pressure is the same for all the conditions. (b) Ventricular volumes waves obtained as the sum of the instantaneous lateral chamber and syringe volumes.

The six P-V loops of step 1, with ESPVR are shown in Fig. 6

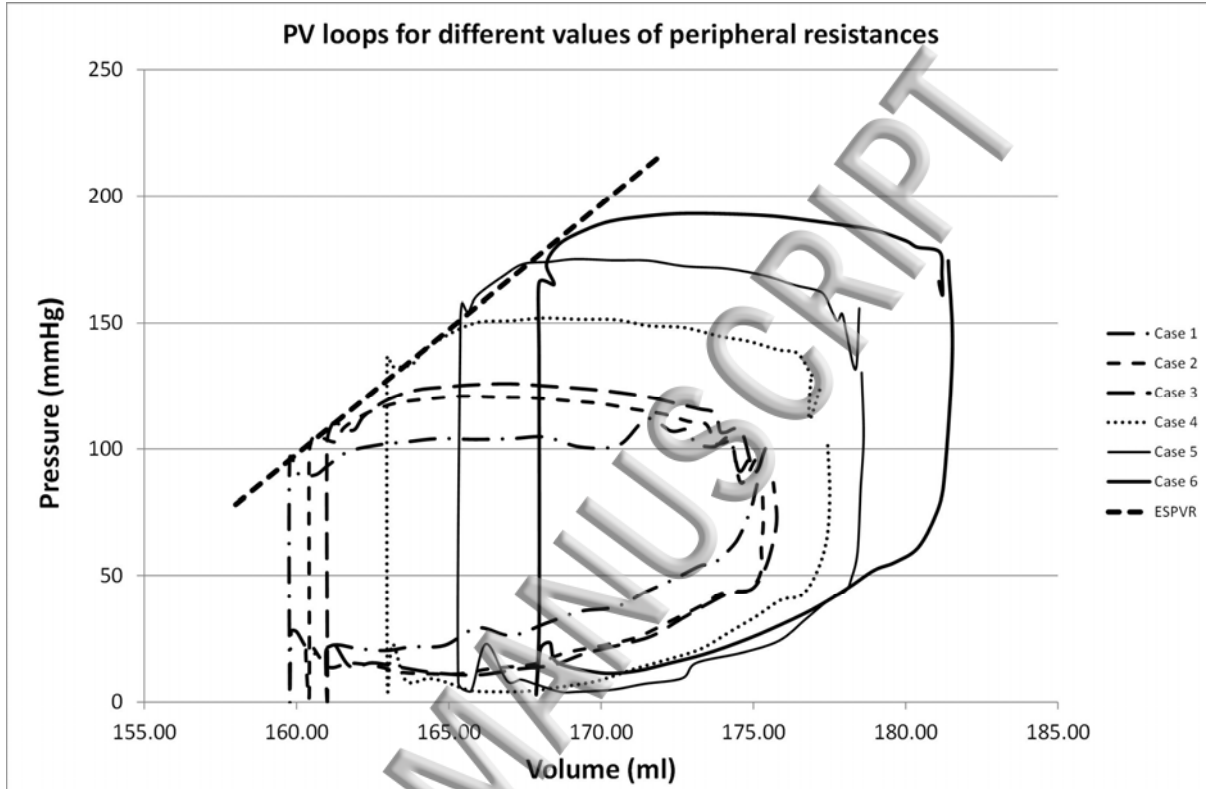


Fig. 6. P-V loops for the considered conditions. Along with the increase in PHR, the end-systolic volume and pressure increase. The best linear interpolation of these points is linear with a squared Pearson's coefficient of 0.98.

The ESPVR was obtained by building the best interpolation line of the values corresponding to the end-systolic phase for each simulated condition. The slope of the line is 9.9 ml/mmHg and the squared Pearson's coefficient is 0.98.

Table 2 shows the values of systolic, diastolic mean pressures and stroke volumes (\pm standard deviations) for the different simulated conditions of step 2.

		R1 (3.9 \pm 0.2) mmHg/ml	R2 (11.5 \pm 0.4) mmHg/ml	R3 (18.2 \pm 0.7) mmHg/ml
V1	<i>SAP (mmHg)</i>	96 \pm 2	166 \pm 3	222 \pm 3
	<i>DAP (mmHg)</i>	35 \pm 3	110 \pm 2	159 \pm 4

	<i>MAP (mmHg)</i>	56±3	129±3	180±4
	<i>SV (ml)</i>	11.2±0.2	8.7±0.1	7.4±0.2
V2	<i>SAP (mmHg)</i>	130±3	207±3	276±3
	<i>DAP (mmHg)</i>	59±4	151±2	221±4
	<i>MAP (mmHg)</i>	83±4	169±3	239±4
	<i>SV (ml)</i>	15.6±0.3	14.0±0.2	13.8±0.3
V3	<i>SAP (mmHg)</i>	152±3	293±3	427±3
	<i>DAP (mmHg)</i>	66±2	210±4	333±2
	<i>MAP (mmHg)</i>	95±3	237±4	364±3
	<i>SV (ml)</i>	21.6±0.3	21.6±0.3	21.6±0.3

Table 2 Pressures and SV values for all the simulated conditions. Each value is represented with the corresponding standard deviation.

For each ventricle, SAP, DAP and MAP increase together with the resistances. For each resistance, the SV increase together with the ventricular elastance: when the ventricle stiffens, more blood flows into the aorta and so the SV is larger. In the last condition (V3), the ventricle is completely stiff so the volume changes are related only to the syringe pumping and are the same for all PHR values. The pressures reached with R2 and R3 are higher than physiological values but the increase is consistent with the corresponding simulated condition and demonstrates the correct behavior of our system.

The P-V loops obtained in the three different ventricular elastance conditions by changing the vascular resistance are shown in Fig. 7.

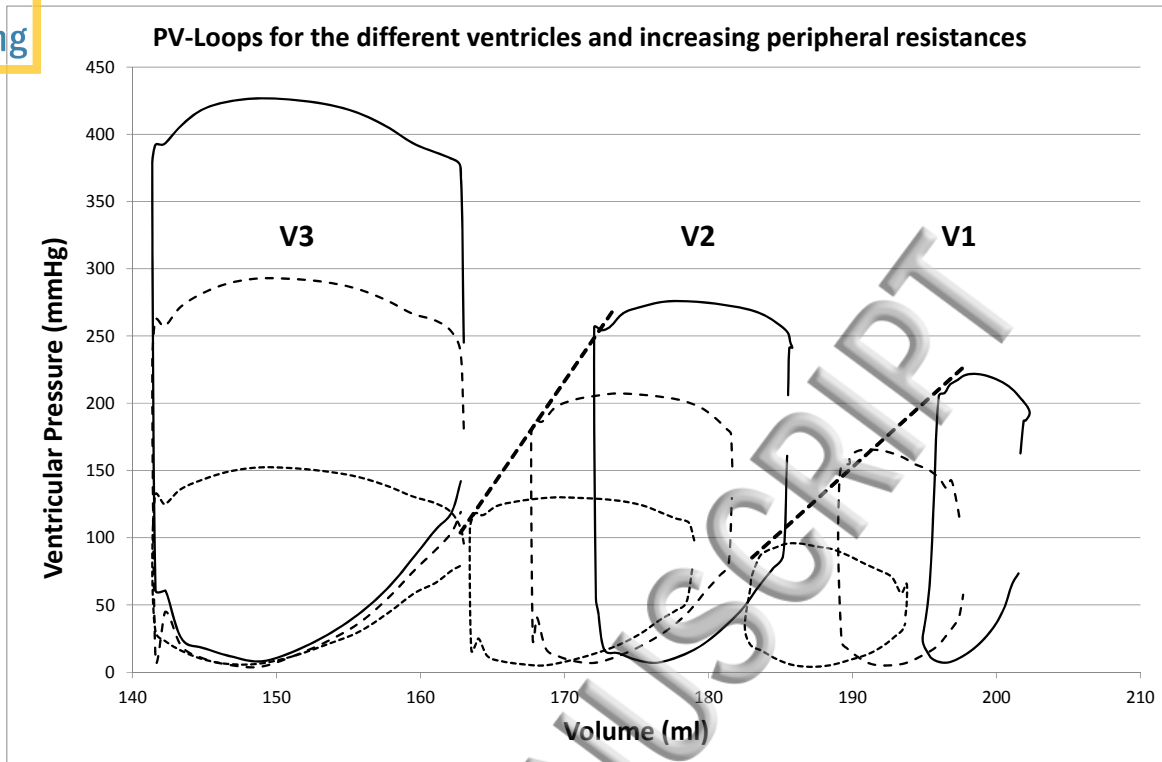


Fig. 7. Ventricular pressure-volume loops in the different simulated conditions.

The ESPVR for V2 and V3 were obtained by building the best interpolation line of the values corresponding to the end-systolic phase for each simulated condition. The slopes of the lines are 9.6ml/mmHg and 15.6ml/mmHg respectively for V1 and V2 (squared Pearson's coefficient of 0.99 for both of them). Since V3 is completely stiff and the volume is fixed, the ESPVR is a vertical line (infinite slope).

Discussion

This paper describes an inexpensive method to transform a fixed stroke alternating syringe ventricle into an adjustable elastance ventricle. It is not a simple solution as it requires the integration of mechanics and computer science, but it simulates pathophysiological conditions which are very difficult or even impossible to obtain on animal preparations. Our proposal is based on the insertion of a lateral chamber of adjustable elastance at the output of a fixed-stroke pumping syringe⁴² and before the aortic valve to simulate (as seen from the aorta) a variable elastance ventricular pump. During the systolic phase, the fluid ejected by the syringe moves to the aorta or to the lateral chamber, depending on their set elastances. The instantaneous "volume" of the ventricle is the sum of that of the syringe

and the lateral chamber, and changes during systole, in relation to both aortic and lateral chamber elastances. All the pressures and flows are monitored and ventricular work production and the efficiency of mechanical energy transfer can be calculated. In physiological mechanical matching, aorta and ventricle have comparable elastance and the energy transfer efficiency is optimal. If the two elastances no longer match, the aorta or the lateral chamber are filled abnormally to simulate pathological conditions like HF, aortic dissection or cardiogenic shock, ventricular hypertrophy, etc. ^{43,44,47-49}.

To change the elastance of both aorta and ventricle, the elastic chambers are inserted inside a rigid cylinder that can be progressively superimposed on the tubes to cause a progressive stiffening of the chamber.

The mock is scaled to mimic a medium-sized animal (dog, small pig, etc.) usually used in experimental surgery laboratories. A higher scale factor would create major problems for the pumping apparatus, valves and elastic tubes. For the validation, the pulse frequency was maintained at quite low values (60 bpm) to facilitate the quantitative evaluations, but a wide range of settings is possible (from 40 to 120 bpm). This could seem a major limitation of our system, but since the settings parameters are maintained constant in time for each condition of ventricular elastance, arterial elastance and peripheral resistances, the results obtained are reliable and can be safely extrapolated to larger animals and humans ^{42,44,47,48,50}.

The basal conditions of elastance and vascular resistance were set to have a physiological shape and values (figure 5) of the aortic pressure pulse for a fixed SV and HR (22ml, 60bpm). The SV was lower (22ml) than that of a normal patient to adapt for the smaller size of the tubes and valves, avoiding turbulence and other undesired phenomena.

The mechanical mock includes a limited Frank-Starling mechanism. This important mechanism acts beat by beat and describes the ability of the heart to change its force of contraction (and therefore the stroke volume) in response to changes in venous return ⁵¹⁻⁵⁴. Since the preload was fixed in each simulated condition, the Frank-Starling mechanism was considered unnecessary to describe the ventricle-arterial coupling and unrelated to the different arterial and aortic elastances.

To test our proposal, in a first step we fixed the elastance of the aorta and ventricle and changed the peripheral resistance in a physiological range. In this way, the mechanical properties of the ventricle are assumed to be unchanged and the ESPVR, built by connecting the end-systolic points of the P-V loops obtained with different resistances,

should lie on a straight line according to the variable elastance ventricular model (Suga and Sagawa) ^{23,25,26,33,37,55}.

As shown in Fig.6, our results are in line with this assumption. This was a good result, but to complete the validation it was necessary to demonstrate that changing the ventricular elastance the slope of the ESPVR changes accordingly (lower elastance = lower slope).

The second step of the research set three different values of ventricular elastance and for each of them the vascular resistance was changed to obtain the ESPVR. Fig. 7 shows the results demonstrating the change in ESPVR slope with ventricular elastance. The group of the first three P-V loops refers to a pure syringe (elastance = ∞) and the ESPVR is vertical. The cases we simulated in the second step of our work cover the extreme range of physiological conditions, thereby demonstrating the hypothesis that the intermediate situations can be easily simulated with the same approach.

With respect to our previous experiment ⁴² in which by changing preload or afterload the P-V loops obtained differed but the ESPVR was the same in all the simulated conditions, the new proposal yields more physiological and accurate results.

Our approach presents two more critical aspects: the first is the dynamic optical measurement of the lateral chamber volume to calculate the instantaneous volume values to build the P-V loop ⁴⁶. The second aspect is the need to adjust the resistance of the line connecting the lateral chamber to the syringe (CLHR) for each change in system parameter (vascular resistance, aortic elastance, lateral chamber elastance, SV, HR). This is mandatory because at the start of syringe ejection the pressure in the lateral chamber and aorta must be the same, otherwise we will have a preferential flow which alters the behaviour. Although these aspects need particular care and attention, they are inexpensive and readily feasible in a research laboratory housing a syringe-like mechanical mock of the cardiovascular system.

In conclusion, a fixed stroke alternating syringe ventricle can be transformed into an adjustable elastance ventricle to study how the mechanical efficiency of energy transfer depends on matching the elastic properties.

Declarations

Competing interests: None declared

Funding: None

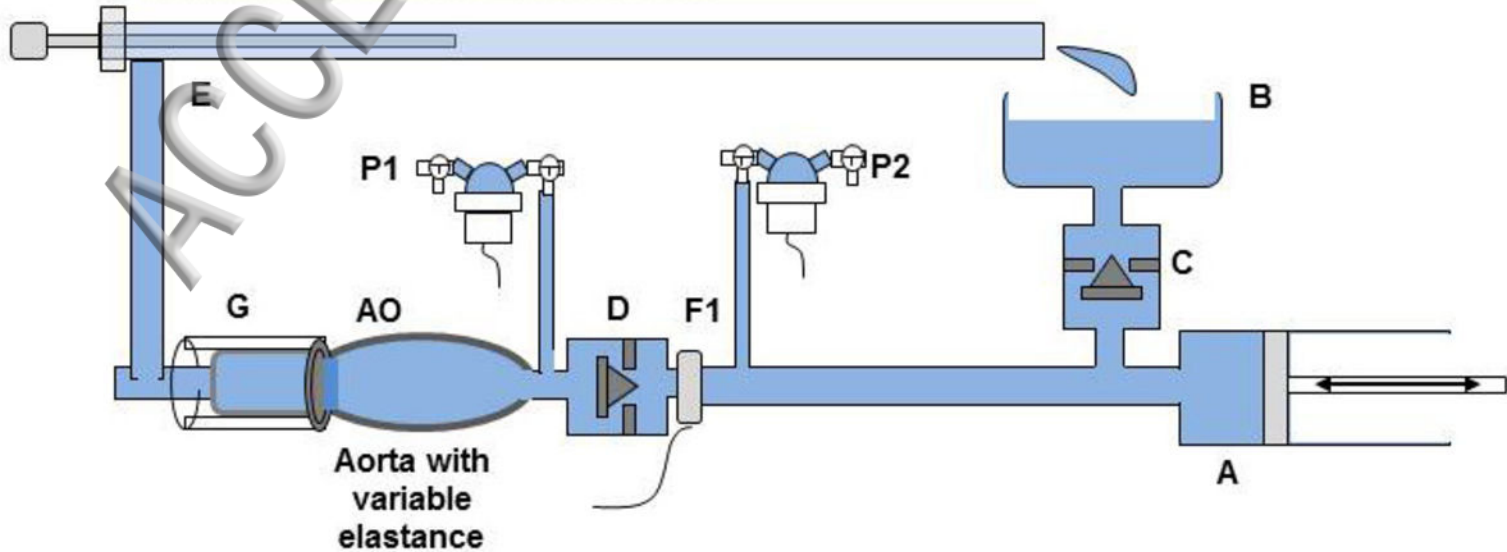
Ethical approval: Not required

References

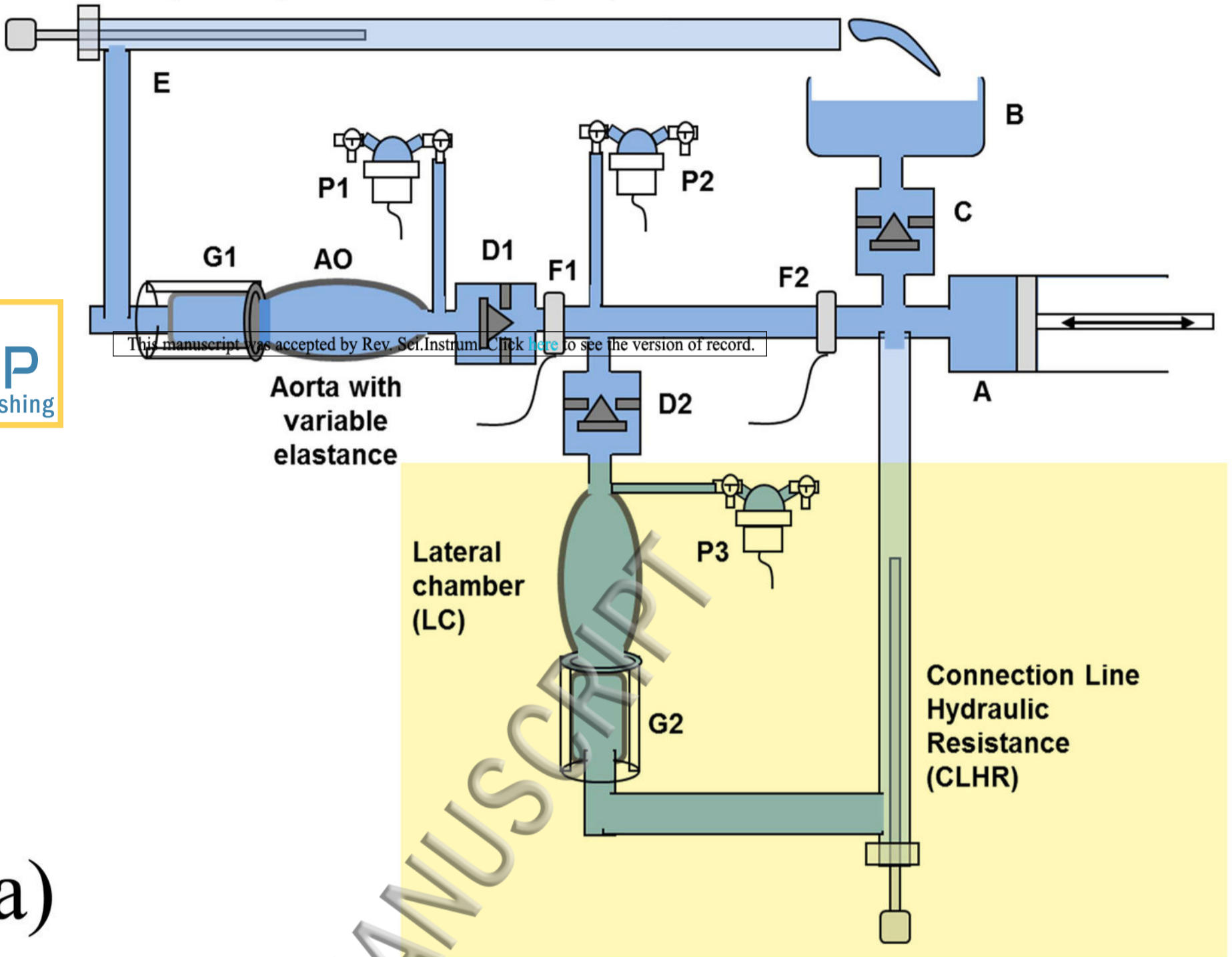
- ¹ A.B. Bhatt, E. Foster, K. Kuehl, J. Alpert, S. Brabeck, S. Crumb, W.R. Davidson, M.G. Earing, B.B. Ghoshhajra, T. Karamlou, S. Mital, J. Ting, Z.H. Tseng, and American Heart Association Council on Clinical Cardiology, *Circulation* **131**, 1884 (2015).
- ² C.S. Rihal, S.S. Naidu, M.M. Givertz, W.Y. Szeto, J.A. Burke, N.K. Kapur, M. Kern, K.N. Garratt, J.A. Goldstein, V. Dimas, T. Tu, Society for Cardiovascular Angiography and Interventions (SCAI), Heart Failure Society of America (HFSA), Society for Thoracic Surgeons (STS), American Heart Association (AHA), and American College of Cardiology (ACC), *Catheter. Cardiovasc. Interv. Off. J. Soc. Card. Angiogr. Interv.* **85**, E175 (2015).
- ³ S.G.-D. Tan, S. Kim, J.K.F. Hon, and H.L. Leo, *PLOS ONE* **11**, e0156580 (2016).
- ⁴ S. Heide-Jørgensen, S. Kumaran Krishna, J. Taborsky, T. Bechsgaard, R. Zegdi, and P. Johansen, *J. Biomech. Eng.* **138**, 034504 (2016).
- ⁵ S. Milo, E. Rambod, C. Gutfinger, and M. Gharib, *Eur. J. Cardio-Thorac. Surg. Off. J. Eur. Assoc. Cardio-Thorac. Surg.* **24**, 364 (2003).
- ⁶ R.S. Heinrich, A.A. Fontaine, R.Y. Grimes, A. Sidhaye, S. Yang, K.E. Moore, R.A. Levine, and A.P. Yoganathan, *Ann. Biomed. Eng.* **24**, 685 (1996).
- ⁷ N.M. Pahlevan and M. Gharib, *J. Biomech.* **46**, 2122 (2013).
- ⁸ A. Ducci, S. Tzamtzis, M.J. Mullen, and G. Burriesci, *J. Heart Valve Dis.* **22**, 688 (2013).
- ⁹ null Yaxin Wang, P.A. Smith, P. De-Sciscio, L.C. Sampaio, W.E. Cohn, null Liping Xu, and R.A. McMahon, *Conf. Proc. Annu. Int. Conf. IEEE Eng. Med. Biol. Soc. IEEE Eng. Med. Biol. Soc. Annu. Conf.* **2017**, 1282 (2017).
- ¹⁰ L. Fresiello, G. Ferrari, A. Di Molfetta, K. Zieliński, A. Tzallas, S. Jacobs, M. Darowski, M. Kozarski, B. Meyns, N.S. Katertsidis, E.C. Karvounis, M.G. Tspirouras, and M.G. Trivella, *J. Biomed. Inform.* **57**, 100 (2015).
- ¹¹ R.A. Chaudhury, V. Atlasman, G. Pathangey, N. Pracht, R.J. Adrian, and D.H. Frakes, *Cardiovasc. Eng. Technol.* (2016).
- ¹² T. Sénage, D. Février, M. Michel, E. Pichot, D. Duveau, S. Tsui, J.N. Trochu, and J.C. Roussel, *ASAIO J. Am. Soc. Artif. Intern. Organs* 1992 **60**, 140 (2014).
- ¹³ X. Zhuang, M. Yang, L. Xu, W. Ou, Z. Xu, F. Meng, and H. Huang, *ASAIO J.* **62**, 410 (2016).
- ¹⁴ O. Bazan and J.P. Ortiz, *Braz. J. Cardiovasc. Surg.* (2016).
- ¹⁵ M.A. Rezaenia, A. Rahideh, B. Alhosseini Hamedani, D.E.M. Bosak, S. Zustiak, and T. Korakianitis, *Artif. Organs* **39**, 502 (2015).
- ¹⁶ D. Timms, M. Hayne, K. McNeil, and A. Galbraith, *Artif. Organs* **29**, 564 (2005).
- ¹⁷ G. Ferrari, C. De Lazzari, R. Mimmo, G. Tosti, D. Ambrosi, and K. Górczyńska, *Int. J. Artif. Organs* **21**, 26 (1998).
- ¹⁸ G. Ferrari, C. De Lazzari, M. Kozarski, F. Clemente, K. Górczyńska, R. Mimmo, E. Monnanni, G. Tosti, and M. Guaragno, *ASAIO J. Am. Soc. Artif. Intern. Organs* 1992 **48**, 487 (2002).
- ¹⁹ F.M. Colacino, F. Moscato, F. Piedimonte, G. Danieli, S. Nicosia, and M. Arabia, *ASAIO J. Am. Soc. Artif. Intern. Organs* 1992 **54**, 563 (2008).
- ²⁰ F.M. Colacino, M. Arabia, G.A. Danieli, F. Moscato, S. Nicosia, F. Piedimonte, P. Valigi, and S. Pagnottelli, *Int. J. Artif. Organs* **28**, 817 (2005).
- ²¹ P. Ruiz, M.A. Rezaenia, A. Rahideh, T.R. Keeble, M.T. Rothman, and T. Korakianitis, *Artif. Organs* **37**, 549 (2013).
- ²² K.-W. Gwak, *Artif. Organs* **39**, 309 (2015).
- ²³ D. Burkhoff, I. Mirsky, and H. Suga, *Am. J. Physiol. Heart Circ. Physiol.* **289**, H501 (2005).
- ²⁴ K.R. Walley, *Crit. Care Lond. Engl.* **20**, 270 (2016).

- ²⁵ H. Suga, A. Kitabatake, and K. Sagawa, *Circ. Res.* **44**, 238 (1979).
- ²⁶ A.P. Voorhees and H.-C. Han, *Compr. Physiol.* **5**, 1623 (2015).
- ²⁷ L. Faconti, R. Bruno, S. Buralli, M. Barzacchi, M. De Luca, L. Ghiadoni, and S. Taddei, *J. Hypertens.* **33 Suppl 1**, e66 (2015).
- ²⁸ L. Faconti, R.M. Bruno, S. Buralli, M. Barzacchi, E. Dal Canto, L. Ghiadoni, and S. Taddei, *JRSM Cardiovasc. Dis.* **6**, 2048004017692277 (2017).
- ²⁹ E. Aslanger, B. Assous, N. Bihry, F. Beauvais, D. Logeart, and A. Cohen-Solal, *J. Am. Heart Assoc.* **4**, e002084 (2015).
- ³⁰ E. Vizzardi, E. Sciatti, I. Bonadei, A. D'Aloia, L. Tartière-Kesri, J.-M. Tartière, A. Cohen-Solal, and M. Metra, *Clin. Res. Cardiol. Off. J. Ger. Card. Soc.* **104**, 1078 (2015).
- ³¹ A. Milan, E. Avenatti, D. Naso, and F. Veglio, *J. Cardiovasc. Echography* **23**, 102 (2013).
- ³² P. Wohlfahrt, M.M. Redfield, V. Melenovsky, F. Lopez-Jimenez, R.J. Rodeheffer, and B.A. Borlaug, *Eur. J. Heart Fail.* **17**, 27 (2015).
- ³³ K.R. Walley, *Crit. Care Lond. Engl.* **20**, 270 (2016).
- ³⁴ V. Bell, E.L. McCabe, M.G. Larson, J. Rong, A.A. Merz, E. Osypiuk, B.T. Lehman, P. Stantchev, J. Aragam, E.J. Benjamin, N.M. Hamburg, R.S. Vasan, G.F. Mitchell, and S. Cheng, *J. Am. Heart Assoc.* **6**, (2017).
- ³⁵ A. Sonaglioni, M. Baravelli, M. Lombardo, C. Sommese, C. Anzà, J.A. Kirk, and L. Padeletti, *Aging Clin. Exp. Res.* (2017).
- ³⁶ F. Loeper, J. Oosterhof, M. van den Dorpel, D. van der Linde, Y. Lu, E. Robertson, B. Hambly, and R. Jeremy, *J. Am. Heart Assoc.* **5**, (2016).
- ³⁷ F. Khalafbeigui, H. Suga, and K. Sagawa, *Am. J. Physiol.* **237**, H566 (1979).
- ³⁸ R. Erbel, V. Aboyans, C. Boileau, E. Bossone, R.D. Bartolomeo, H. Eggebrecht, A. Evangelista, V. Falk, H. Frank, O. Gaemperli, M. Grabenwöger, A. Haverich, B. Jung, A.J. Manolis, F. Meijboom, C.A. Nienaber, M. Roffi, H. Rousseau, U. Sechtem, P.A. Sirnes, R.S. von Allmen, C.J.M. Vrints, and ESC Committee for Practice Guidelines, *Eur. Heart J.* **35**, 2873 (2014).
- ³⁹ M.A. Fifer, C.N. Aroney, M.J. Semigran, H.C. Herrmann, G.W. Dec, and C.A. Boucher, *Am. Heart J.* **119**, 451 (1990).
- ⁴⁰ L.A. Baloa, J.R. Boston, and J.F. Antaki, *Ann. Biomed. Eng.* **29**, 244 (2001).
- ⁴¹ G. Ferrari, C. De Lazzari, R. Mimmo, D. Ambrosi, and G. Tosti, *J. Med. Eng. Technol.* **18**, 87 (1994).
- ⁴² R. Zannoli, I. Corazza, and A. Branzi, *Phys. Med.* **25**, 94 (2009).
- ⁴³ R. Zannoli, I. Corazza, A. Branzi, and P.L. Rossi, *J. Mech. Med. Biol.* **8**, 109 (2008).
- ⁴⁴ I. Corazza, D. Bianchini, E. Marcelli, L. Cercenelli, and R. Zannoli, *J. Biomech.* **47**, 1618 (2014).
- ⁴⁵ I. Corazza, G. Barletta, P. Guaraldi, A. Cecere, G. Calandra-Buonaura, E. Altini, R. Zannoli, and P. Cortelli, *Comput. Methods Programs Biomed.* **117**, 267 (2014).
- ⁴⁶ I. Corazza, L. Casadei, and R. Zannoli, *Biomed. Signal Process. Control* **33**, 255 (2017).
- ⁴⁷ I. Corazza, G. Melandri, S. Nanni, E. Marcelli, L. Cercenelli, D. Bianchini, F. Vagnarelli, and R. Zannoli, *J. Mech. Med. Biol.* **13**, UNSP 1340004 (2013).
- ⁴⁸ R. Zannoli, I. Corazza, A. Cremonesi, and A. Branzi, *J. Biomech.* **40**, 3089 (2007).
- ⁴⁹ I. Corazza, C. Pinardi, L. Manco, D. Bianchini, L. Cercenelli, E. Marcelli, and R. Zannoli, *J. Mech. Med. Biol.* **13**, UNSP 1340005 (2013).
- ⁵⁰ R. Zannoli, I. Corazza, P. Cacciafesta, and A. Branzi, *J. Mech. Med. Biol.* **5**, 369 (2005).
- ⁵¹ R. Jacob and G. Kissling, *Basic Res. Cardiol.* **84**, 227 (1989).
- ⁵² R.H. Schwinger, M. Böhm, A. Koch, U. Schmidt, I. Morano, H.J. Eissner, P. Uberfuhr, B. Reichart, and E. Erdmann, *Circ. Res.* **74**, 959 (1994).
- ⁵³ V. Sequeira and J. van der Velden, *Biophys. Rev.* **9**, 259 (2017).
- ⁵⁴ R. Zannoli, S. Sorbello, I. Corazza, G. Pepe, G. Lepera, and A. Branzi, *J. Mech. Med. Biol.* **2**, 177 (2002).
- ⁵⁵ H. Suga, *Front. Med. Biol. Eng. Int. J. Jpn. Soc. Med. Electron. Biol. Eng.* **2**, 3 (1990).

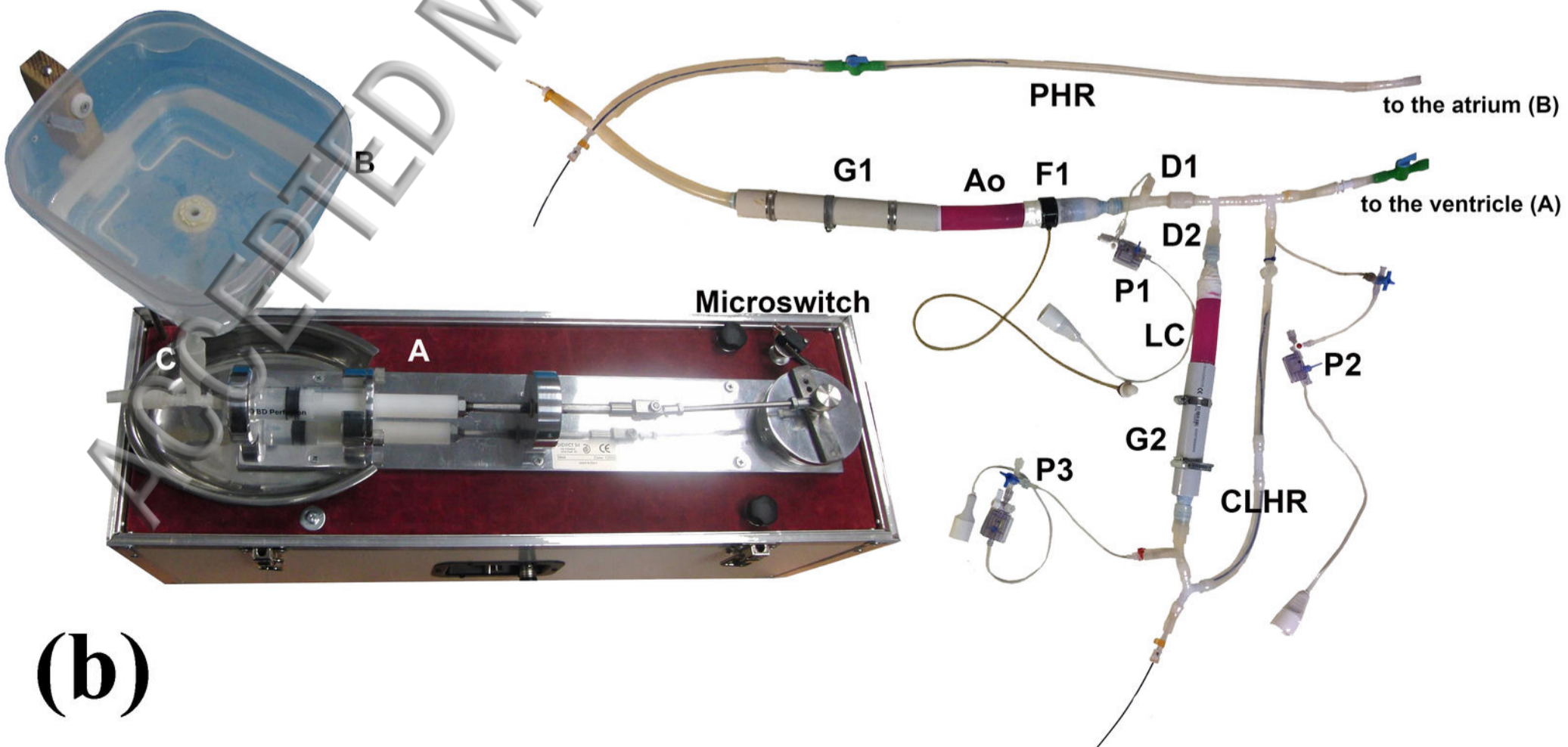
Peripheral Hydraulic Resistance (PHR)



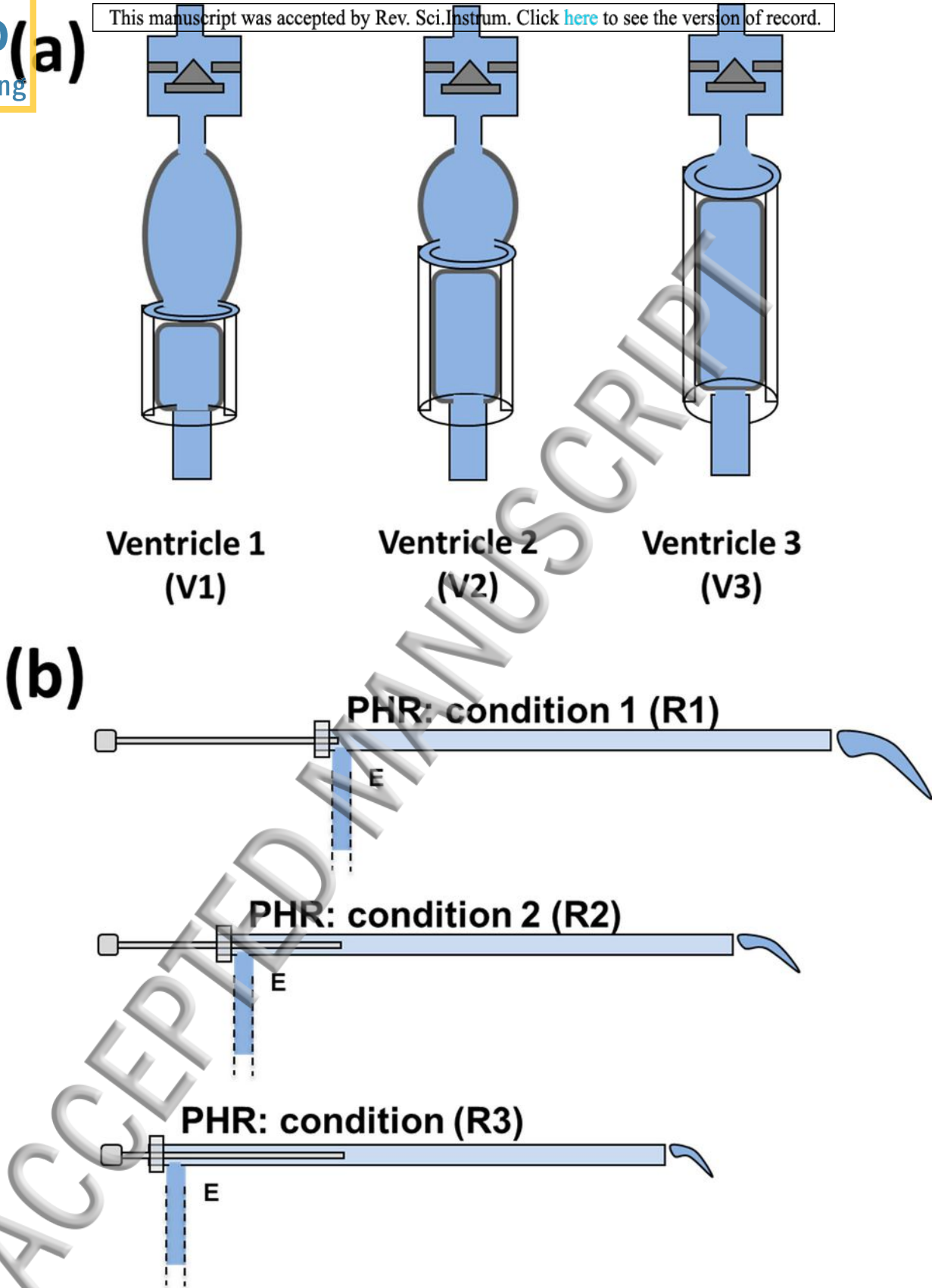
Peripheral Hydraulic Resistance (PHR)

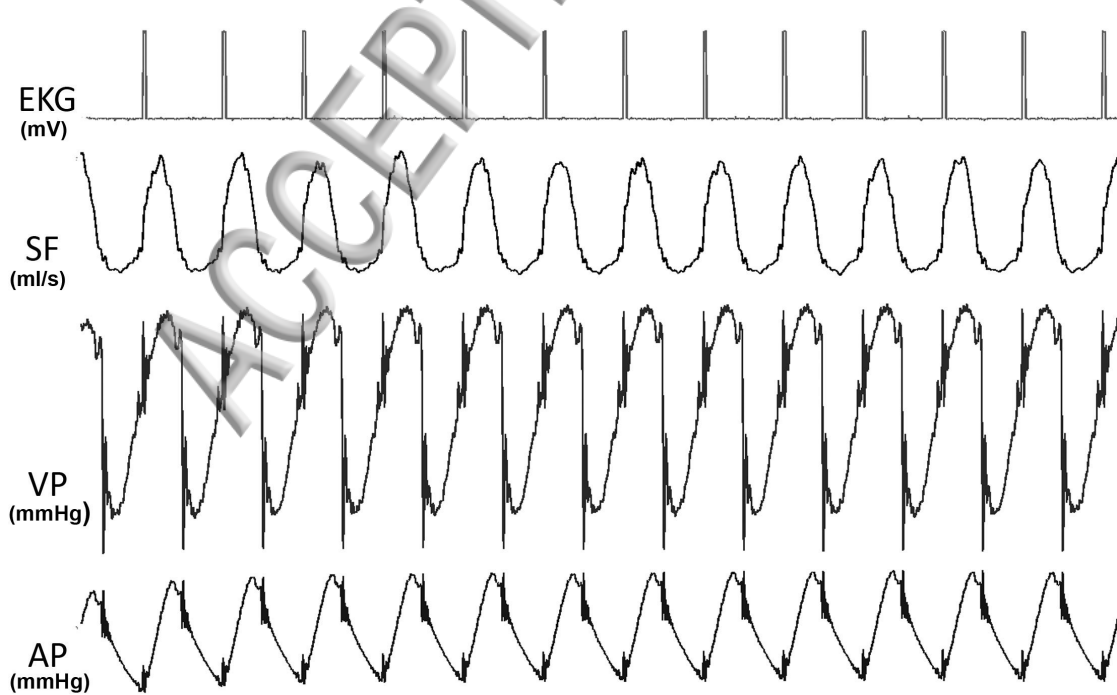


(a)



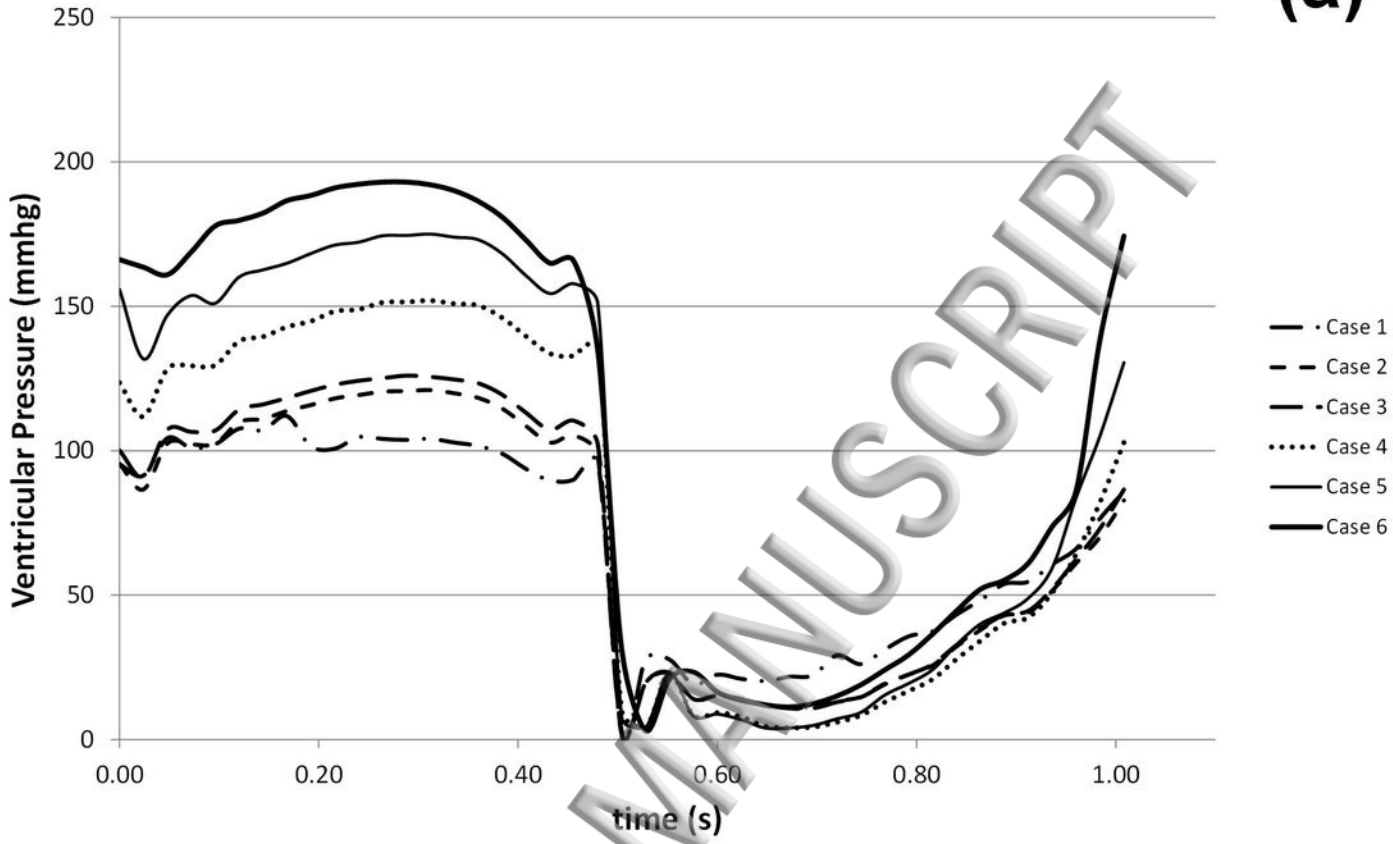
(b)





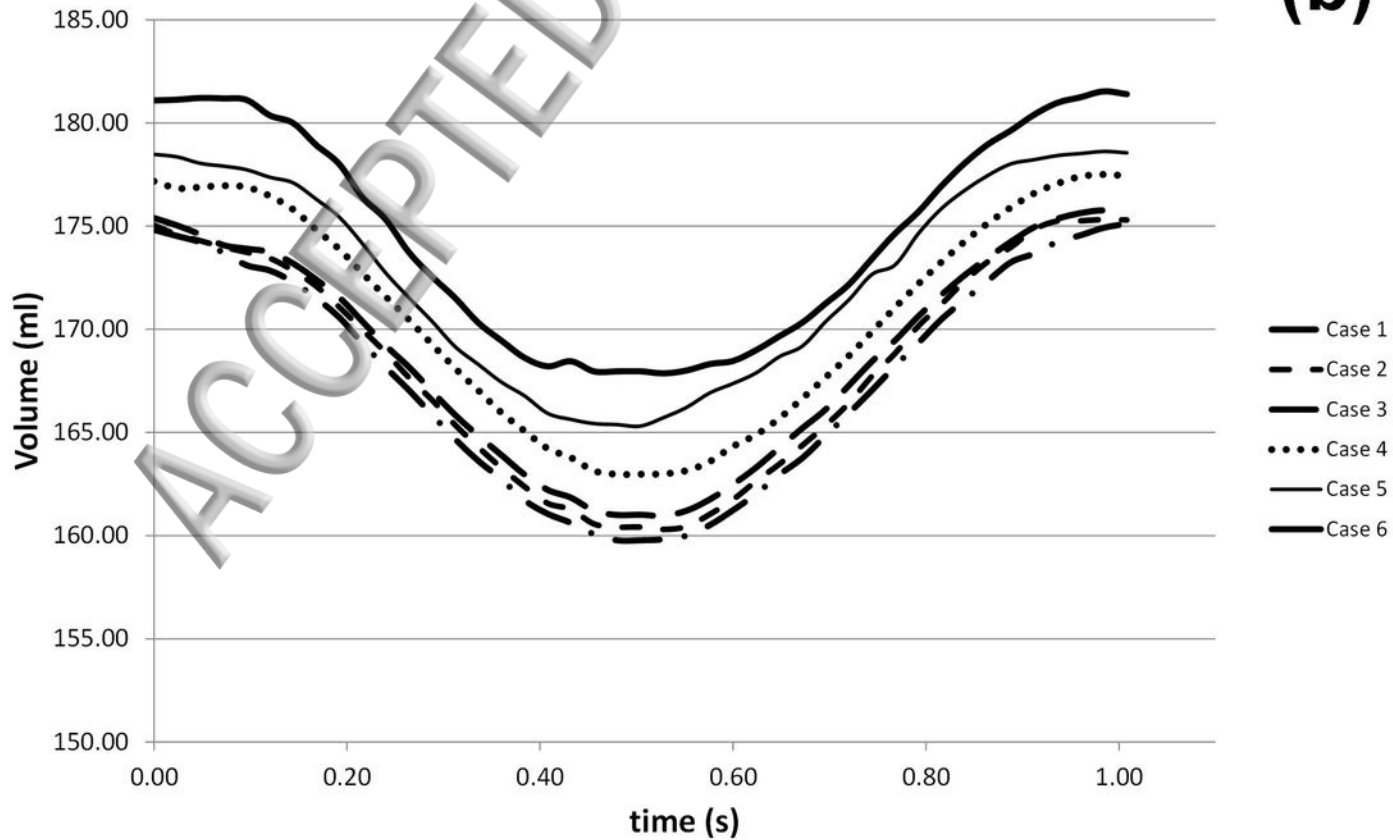
Ventricular pressure waves for the different conditions

(a)

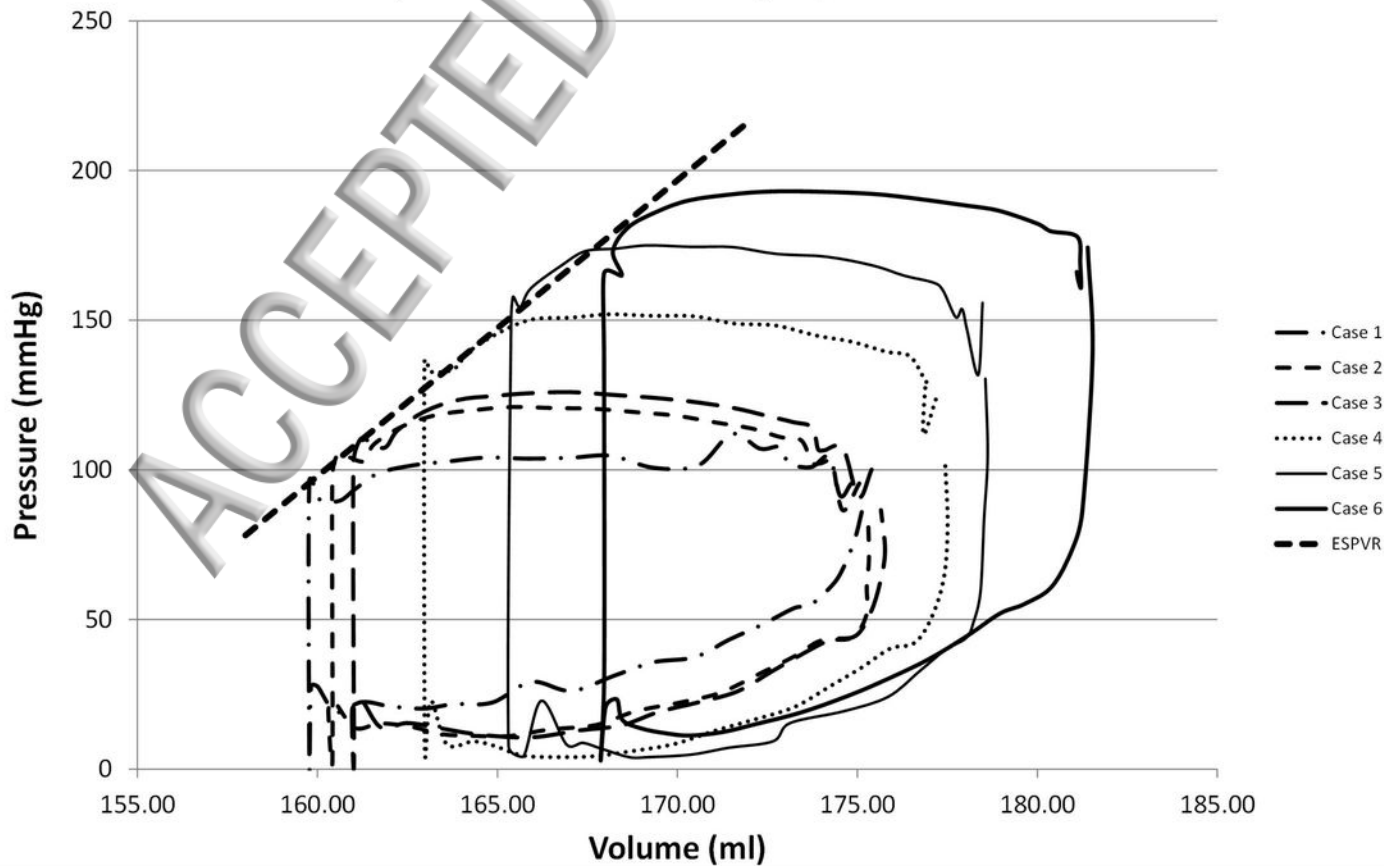


Ventricular volumes for the different conditions

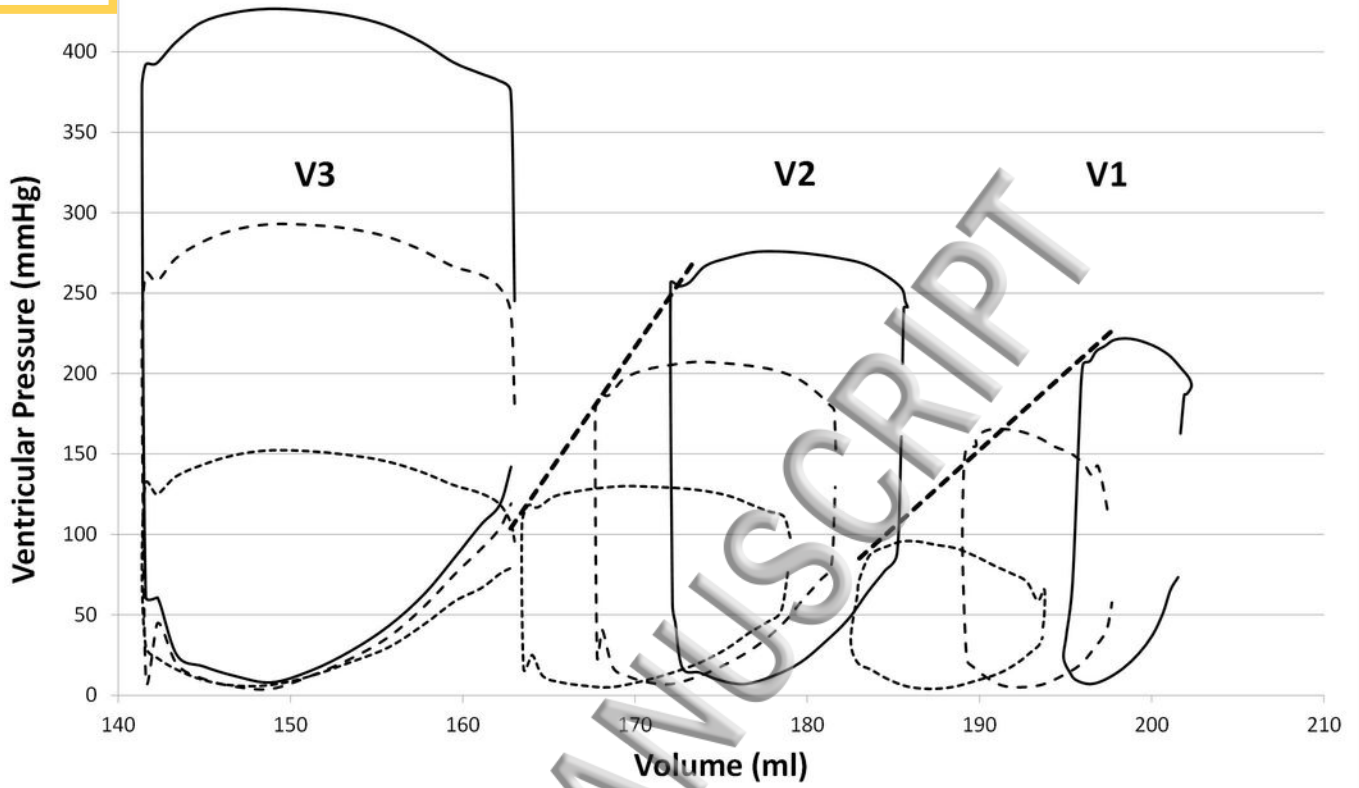
(b)



PV loops for different values of peripheral resistances



PV-Loops for the different ventricles and increasing peripheral resistances



ACCEPTED MANUSCRIPT